

# Crystal transition mechanisms in poly(ethylene succinate)

Y. Ichikawa<sup>a,1,2,\*</sup>, K. Noguchi<sup>a</sup>, K. Okuyama<sup>a</sup>, J. Washiyama<sup>b</sup>

<sup>a</sup>Faculty of Technology, Tokyo University of Agriculture and Technology, Koganei, Tokyo 184-8588, Japan

<sup>b</sup>Kawasaki Development Center, Montell-SDK-Sunrise Co., Ltd, 2-3-2, Yako, Kawasaki-ku, Kawasaki 210-8548, Japan

Received 5 June 2000; received in revised form 8 September 2000; accepted 18 September 2000

## Abstract

Poly(ethylene succinate) [PES] showed a crystal transition between the  $\alpha$  ( $T_3GT_3\bar{G}$ ) and  $\beta$  ( $T_8$ ) form, where T, G and  $\bar{G}$  denoted *trans*, *gauche* and minus *gauche*, respectively. Here, the  $\beta$  form appeared only under the strain. We have investigated the mechanisms of this crystal transition by FT-IR and X-ray diffraction. In the FT-IR spectrum, the absorbance peaks at 841 and 873  $\text{cm}^{-1}$ , corresponding to the  $\alpha$  form, started decreasing at strain of  $\epsilon \sim 20\%$ , while the absorbance at 805  $\text{cm}^{-1}$ , corresponding to the  $\beta$  form, appeared at  $\epsilon \sim 20\%$ , then increased with strain. In addition, the isosbestic point was observed at 820  $\text{cm}^{-1}$ , indicating that the crystal transition occurred only between the  $\alpha$  and  $\beta$  form, where no amorphous part contributed. In the X-ray diffraction, streaks appeared in layer lines in the  $\beta$  form, indicating that the  $\beta$  form had some disorder along the fiber axis. The equatorial reflection of  $\alpha$  (at  $2\theta = 20.4^\circ$ ) started decreasing at  $\epsilon \sim 15\%$ . On the other hand, the reflection of  $\beta$  (at  $2\theta = 21.9^\circ$ ) appeared at  $\epsilon \sim 15\%$ , then increased with  $\epsilon$ , consistent with FT-IR results. The molar fraction of the  $\beta$  form,  $\chi_\beta$ , was determined as a function of stress,  $\sigma$ , by X-ray, where  $\chi_\beta$  showed a drastic increase at a critical value of  $\sigma^* = 190$  MPa. The thermodynamic first-order phase transition was hence the operative mechanism of the transition as similar to poly(butylene terephthalate) [PBT] and poly(tetramethylene succinate) [PTMS]. The free energy difference between the  $\alpha$  and  $\beta$  form,  $\Delta G$ , was determined to be  $\Delta G \sim 2.3$  (kJ/mol of monomer unit), being larger than the reported value of PBT ( $\Delta G \sim 1.4$ ) and PTMS ( $\Delta G \sim 1.6$ ). This difference would arise from the locus of conformational change upon the transition. In the case of PES, the conformational change was observed in both alcohol and acid units, while in the cases of PTMS and PBT, it was observed in the alcohol unit. © 2001 Elsevier Science Ltd. All rights reserved.

**Keywords:** Crystal transition mechanism; Biodegradable polymer; Poly(ethylene succinate)

## 1. Introduction

Strain induced crystal modifications have been reported in several polyesters, such as in poly(butylene terephthalate) (PBT) [1–11] and poly(tetramethylene succinate) (PTMS) [12–14]. In PBT, for instance, two kinds of crystal modifications ( $\alpha$  and  $\beta$  form) have been reported. Here, the  $\beta$  form appeared only under strain. Yokouchi et al. [4] and Hall et al. [5] independently determined the crystal structures of the  $\alpha$  and  $\beta$  form of PBT. In the case of PTMS [12–14], crystal modifications ( $\alpha$  and  $\beta$  form) have also been reported, where the  $\beta$  form appeared under strain. The authors determined the crystal structures of the both forms [14,15]. The crystal structure of poly(ethylene succinate) [PES] has been reported ( $\alpha$  form) [16].

Recently, the authors have discovered new crystal modification ( $\beta$  form) of PES. The transition occurred under application or removal of strain [17]. Conformations of these two forms were reported to be ( $T_3GT_3\bar{G}$ ) [16,17] and ( $T_8$ ) [17] for the  $\alpha$  and  $\beta$  form, respectively. It should be noted that streaks appeared in the layer lines of the  $\beta$  form of PES upon the crystal transition [17], while no streaks were observed in the  $\beta$  form of PBT and PTMS.

The crystal transition mechanisms were investigated and well established in PBT [7] and in PTMS [13] as well as in poly(ethylene oxide) (PEO) [18]. These studies showed that these crystal transitions belong to the thermodynamic first-order phase transition. The mechanism accounted well for the observations: (1) The fraction of the  $\beta$  form showed a discontinuous change at a certain level of stress; (2) The existence of a plateau in a stress–strain curve. The authors thus principally focused on the crystal transition mechanisms in PES with a special emphasis on the comparison to those reported in PTMS and PBT.

\* Corresponding author. Tel.: +81-44-277-7186; fax: +81-44-299-2763.

E-mail address: ichikawa@kpl.sdk.co.jp (Y. Ichikawa).

<sup>1</sup> Present address: Kawasaki Plastics Laboratory, Showa Denko K.K., 3-2, Chidori-cho, Kawasaki-ku, Kawasaki 210-0865, Japan.

<sup>2</sup> On leave from Showa Denko K.K. Kawasaki Plastics Laboratory.

## 2. Experimental section

### 2.1. Materials

PES, so called Bionolle, was supplied in a commercial pellet form from Showa Highpolymer Co. Ltd; no further purification was made on the polymer. The weight average molecular weight was determined to be  $1.6 \times 10^5$  by size exclusion chromatography with poly(methylmethacrylate) standards. The melting ( $T_m$ ) and glass transition temperatures ( $T_g$ ) were measured to be 99 and  $-11^\circ\text{C}$ , respectively (by DSC).

### 2.2. Sample preparation

Uniaxially oriented fibers were fabricated [12–15,17]; these fiber specimens were utilized in the following X-ray studies. Film specimens were also prepared under the identical thermal conditions for FT-IR studies.

### 2.3. X-ray measurements

A rotating-anode X-ray generator (RU-200, Rigaku) was operated in a normal focus mode to provide a monochromatized X-ray beam. We used beam source,  $\text{CuK}\alpha$ ,  $\lambda = 0.15418$  nm operated at  $50 \text{ kV} \times 140 \text{ mA}$ . Diffraction data were recorded on a disk-shaped imaging plate with the sample-plate distance of 150 mm. The diffraction pattern was read by measuring the fluorescence intensity stimulated by a focused He–Ne laser beam that scanned spirally the surface of the imaging plate. The measurement of X-ray diffraction data was implemented by the hardware system, DIP100S (MAC Science). Wide angle X-ray diffractions were measured at room temperature under various strains between 0 and 35%, where the stepwise strains were applied to and removed from the fiber. The diffraction curve for each strain was obtained 30 min after the application of the strain: we have confirmed the stress to reach an equilibrium value and remained constant ( $\sim 85\%$  of the initial stress) under this condition. The equatorial reflections were used to evaluate the ratio of the  $\beta$  form.

X-ray fiber photographs were also taken for both the original and strained (by 35%) fibers by means of a cylindrical camera (diameter of 100 mm) as reported previously [17].

Small angle X-ray diffraction was measured to determine the long period,  $L_0$ . Wide angle diffraction was also measured for the determination of the crystallite size,  $L_{cr}$ , along the drawing direction using 004 reflection from the  $\alpha$  form based on the Scherrer equation [19]: the correction of the slit width was made using Si.

### 2.4. FT-IR measurements

FT-IR spectra of PES were obtained at room temperature under stepwise strains as described in the above. We mainly focused on the absorbance peaks at  $873$  and  $841 \text{ cm}^{-1}$  (for

the  $\alpha$  form) and the peak at  $805 \text{ cm}^{-1}$  (for the  $\beta$  form): these peaks disappeared in a molten state.

## 3. Results and discussion

### 3.1. FT-IR spectra

The FT-IR spectra of PES under various strains are shown in Fig. 1. The absorbance peaks at  $873$  and  $841 \text{ cm}^{-1}$  start decreasing at strain of  $\epsilon \sim 20\%$ , while the peak at  $805 \text{ cm}^{-1}$  appears at this strain. These observations indicate that the peaks at  $873$  and  $841 \text{ cm}^{-1}$  correspond to the  $\alpha$  form crystal, and the peak at  $805 \text{ cm}^{-1}$  is assigned to the  $\beta$  form. It is worthwhile to point out that the spectra have an isosbestic point at  $820 \text{ cm}^{-1}$ . Similar kind of an isosbestic point was reported in PBT [7] and PTMS [13]. The existence of the isosbestic point indicates that the crystal transition occurs only between the  $\alpha$  form and the  $\beta$  form, where no amorphous part is transformed into crystal [6,7]. It would thus be possible to evaluate the molar fraction of the  $\beta$  form,  $\chi_\beta$ , as a function of  $\epsilon$  [7,13,18]. As pointed out earlier, the FT-IR spectra includes some ambiguity in the quantitative interpretation of the data [7,13]. We hence employ X-ray diffraction method hereafter for more quantitative analyses, where only the signals from crystal phase can be extracted [13].

### 3.2. X-ray diffraction

The X-ray fiber photographs for the  $\alpha$  ( $\epsilon = 0\%$ ) and  $\beta$  ( $\epsilon = 35\%$ ) forms are shown in Fig. 2. The reflection spots indicated by the arrows are used for the later analyses. X-ray diffraction profiles of equator under various strains are plotted in Fig. 3. Two well-defined reflection peaks at  $2\theta = 20.4^\circ$  and  $2\theta = 21.9^\circ$  are assigned to  $\alpha$ , 120, and  $\beta$  forms, respectively. It should be noted that the intensity of the reflection at  $2\theta = 20.4^\circ$  starts decreasing at  $\epsilon \sim 15\%$ ,

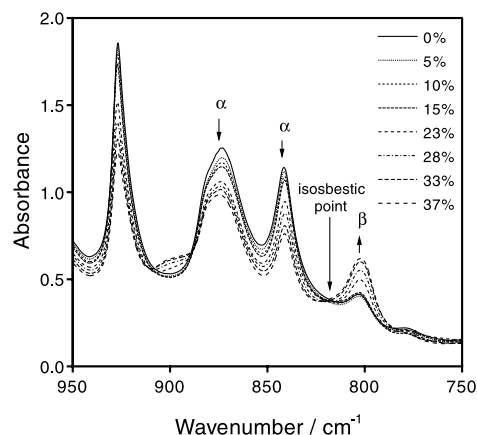


Fig. 1. FT-IR spectra under various strains (0–37%) are shown. Note that the absorbance peaks at  $873$  and  $841 \text{ cm}^{-1}$  start decreasing at  $\epsilon = 20\%$  (broken line), while the peak at  $805 \text{ cm}^{-1}$  appears at  $\epsilon = 20\%$  then increases with strain. The existence of the isosbestic point at  $820 \text{ cm}^{-1}$  should also be noted.

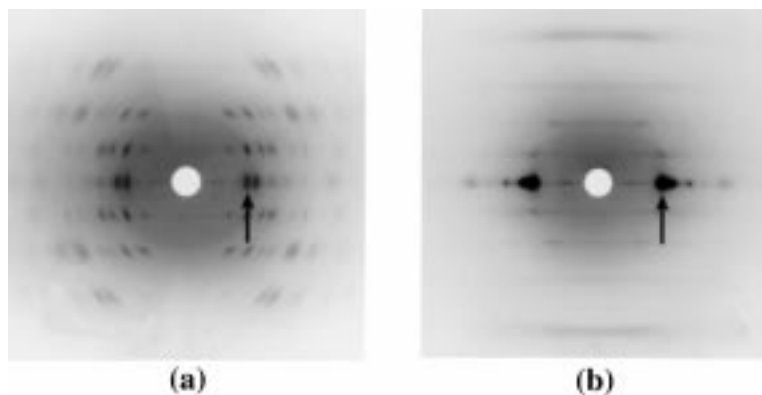


Fig. 2. The X-ray fiber photographs are shown: (a) for the  $\alpha$  form ( $\epsilon = 0\%$ ); (b) for the  $\beta$  form ( $\epsilon = 35\%$ ). Note that streaks in layer lines can be seen in the latter case.

while the reflection at  $2\theta = 21.9^\circ$  appears at  $\epsilon \sim 15\%$  then increases with  $\epsilon$ . In addition, the change is reversible with respect to the repeated application and removal of stain. These observations are substantially consistent with the FT-IR results.

The above two equatorial reflections are thus used for the determination of  $\chi_\beta$ . The details of the procedure are described in below. First, the integrated intensity of the 120 reflection of the  $\alpha$  form ( $2\theta = 20.4^\circ$ ),  $I_\alpha$ , is plotted with respect to the intensity of the reflection of  $\beta$  form ( $2\theta = 21.9^\circ$ ),  $I_\beta$ , for each strain in Fig. 4, where the data points fall on a single straight line with a slope of  $1/a$  (Note that the  $a$  is negative.). Then  $\chi_\beta$  is calculated via Eq. (1) [10,20].

$$\chi_\beta = I_\beta / (I_\beta - aI_\alpha) \quad (1)$$

The  $\chi_\beta$  is thereby plotted as a function of  $\epsilon$  in Fig. 5a. The  $\chi_\beta$  starts increasing at  $\epsilon \sim 12\%$  and shows a drastic increase with increasing  $\epsilon$ , then, almost saturates at  $\epsilon \sim 25\%$ . These observations indicate that the transition occurs between  $\epsilon \sim 12\%$  and  $\epsilon \sim 25\%$ . The transition behaviors observed by FT-IR and X-ray in this study are thus essentially the same as those observed in PBT [7] and PTMS [13]. In order

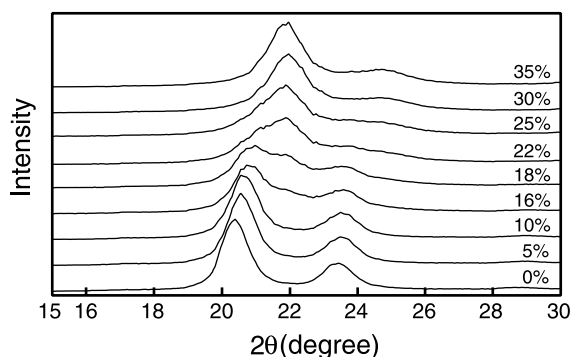


Fig. 3. The equatorial reflection curves are shown. The reflection peaks at  $2\theta = 20.4^\circ$  and  $2\theta = 21.9^\circ$  correspond to the  $\alpha$  and  $\beta$  reflections, respectively. Note that the  $\alpha$  reflection starts decreasing at  $\epsilon \sim 15\%$ , while the  $\beta$  reflection appears at  $\epsilon \sim 15\%$  then increases with strain.

to evaluate the critical stress ( $\sigma^*$ ) of the transition, the  $\chi_\beta$  vs. strain ( $\epsilon$ ) plot is converted into  $\chi_\beta$  vs. stress ( $\sigma$ ) (see Fig. 5b), from the relationship between  $\epsilon$  and an equilibrium value of  $\sigma$  at each  $\epsilon$  [13].

### 3.3. Streaks in layer lines

Streaks in layer lines appear in the  $\beta$  form as shown in Fig. 2, which indicates that the  $\beta$  form of PES contains disorder along the chain axis: the streaks do not disappear after annealing at  $80^\circ\text{C}$  for 12 h. Such streaks in layer line are also reported in poly( $\beta$ -methyl- $\beta$ -propiolactone) [21]. Similarity of the size and symmetry of methylene and carbonyl groups may result in such a disorder in the molecular arrangement [22]. In the case of PTMS, no streaks in layer lines can be observed [12]. Tsuji et al. however, have reported that the  $\beta$  form of PTMS showed streaks during elongation and that the streaks disappeared after anneal at  $107^\circ\text{C}$  [23,24]. The specimen that Tsuji et al., used was not

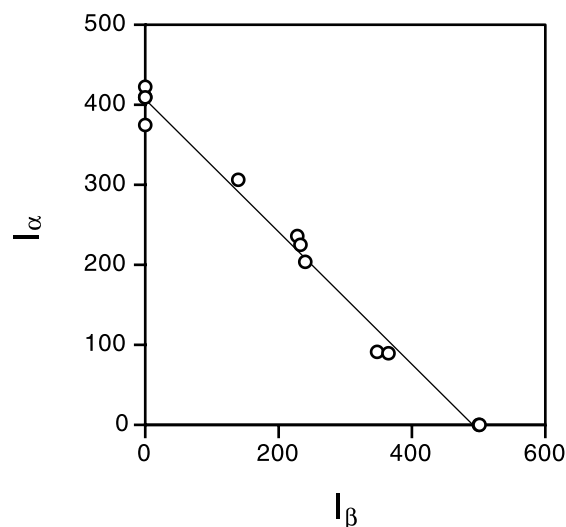


Fig. 4. The integrated intensity of the reflection at  $2\theta = 20.4^\circ$ ,  $I_\alpha$ , is plotted with respect to that at  $2\theta = 21.9^\circ$ ,  $I_\beta$ . Note that the data points fall on a single straight line.

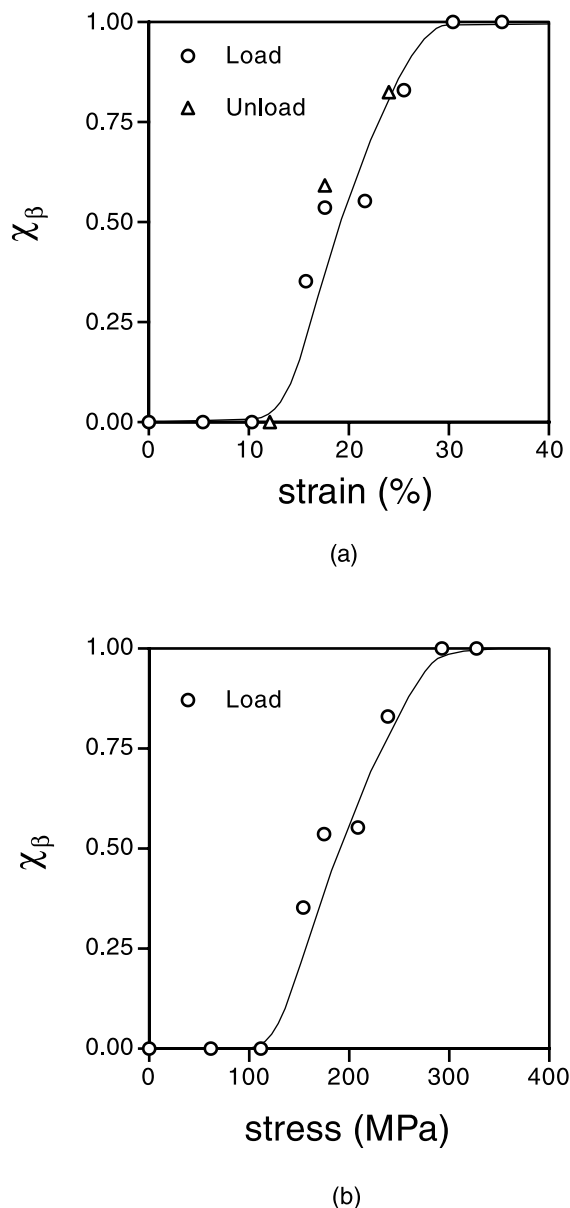


Fig. 5. The  $\chi_\beta$ , obtained by X-ray, is plotted as a function of (a) strain and (b) stress. Note that  $\chi_\beta$  starts increasing at  $\epsilon \sim 12\%$  then saturates at  $\epsilon \sim 25\%$ .

annealed before the formation of the  $\beta$  form. On the other hand, the specimens for the present study is a uniaxially oriented fiber (the  $\alpha$  form of PTMS) that is well annealed. The former specimens would thus contain more defects.

It seems likely that the initial structure, and hence  $\alpha$  form, would dictate the structure after the transition ( $\beta$  form). The position of the C=O group along the chain axis is almost equal to those of surrounding chains in the  $\alpha$  form of PTMS [14,15]. The molecular packing around the C=O group would thus be a closed packing. In the course of the transition between the  $\alpha$  and  $\beta$  form, the structural change occurs in the tetramethylene units. The relative position against the surrounding chains are maintained even upon the crystal transition to the  $\beta$  form. On the other hand, in

the  $\alpha$  form of PES [16] and poly( $\beta$ -methyl- $\beta$ -propiolactone) [21], the position of the C=O group along the chain axis against those of the surrounding chains has off-set, allowing to cause the displacement of chains with respect to the surrounding chains in the crystal upon crystal transition under stress. In such a circumstance, it is unlikely that the displacement takes place identically, which introduces disorder along the fiber axis in the  $\beta$  form. Hence streaks in layer lines can be observed in PES [17] and poly( $\beta$ -methyl- $\beta$ -propiolactone) [21] as opposed to PTMS [12–14].

It is important to note that the streaks in layer lines of PES disappear when the stress is removed as opposed to the case in poly( $\beta$ -methyl- $\beta$ -propiolactone), where the streaks remain after the removal of stress [21].

### 3.4. Crystal transition mechanisms

Two different models have been proposed for the crystal transition mechanisms: one is the kinetic model and the other is the thermodynamic first-order phase transition model. In the former model,  $\chi_\alpha$  and  $\chi_\beta$  are determined by the reaction rates (from  $\alpha$  to  $\beta$  and vice versa), i.e. the free energy barrier between  $\alpha$  and  $\beta$ . Consequently, the plot  $\ln(\chi_\beta/\chi_\alpha)$  vs.  $\sigma$  should fall on a single straight line [25,26]. In the latter model,  $\chi_\alpha$  as a function of  $\sigma$  should show a discontinuous jump at a certain value of  $\sigma$  ( $=\sigma^*$ : critical stress) [7,13,18]. These two kinds of plots therefore make it possible to determine the crystal transition mechanism. In the case of PES, the  $\ln(\chi_\beta/\chi_\alpha)$  vs.  $\sigma$  does not fall on a single straight line at all, ruling out the kinetic model. On the other hand, the  $\chi_\beta$  shows a drastic increase at around  $\sigma \sim 190$  MPa (see Fig. 5b). These observations indicate that the crystal transition mechanism in PES is the thermodynamic first-order phase transition rather than the kinetic one, similar to those of PBT [7] and PTMS [13].

### 3.5. The critical stress

The critical stress,  $\sigma^*$ , is determined based on the definition that  $\sigma = \sigma^*$  at  $\chi_\beta = 0.5$ , and we thereby obtain  $\sigma^*$  to be about 190 MPa. Since the transition mechanism is the thermodynamic first-order phase transition,  $\sigma^*$  is given by Eq. (2) [7,13]:

$$\sigma^* = \Delta G/[A_\alpha(L_\beta - L_\alpha)] \quad (2)$$

where  $\Delta G$  and  $A_\alpha$  denote the difference in the free energy between the  $\alpha$  and  $\beta$  form per monomer unit and the cross sectional area of the unit cell of the  $\alpha$  form perpendicular to the  $c$ -axis, respectively. The values of such parameters for PTMS and PBT are summarized in Table 1. It should be noted that the  $\Delta G$  of PES (2.3 kJ/mol of monomer unit) is larger than that of PBT (1.4 kJ/mol of monomer unit) [7] or PTMS (1.6 kJ/mol of monomer unit) [13]. Conformation change upon crystal transition takes place in tetramethylene units in both PBT and PTMS. On the other hand, the conformational change takes place in two ethylene units,

Table 1  
Crystal transition parameters for PES, PTMS and PBT

Materials	PES	PTMS	PBT
$\alpha$ form	$T_3GT_3\bar{G}$	$T_7GT\bar{G}$	$\bar{G}\bar{G}TGG$
$\beta$ form	$T_8$	$T_{10}$	TTTTT
$\sigma^*$ (MPa)	190	140	75
$\Delta G$ (kJ/mol <sup>-1</sup> )	2.3	1.6	1.4

ethylene glycol and succinate units, in PES [16]. This difference may cause the value of the free energy  $\Delta G$ . The existence of disorder in the  $\beta$  form results in a positive number of entropy difference,  $\Delta S$ , and hence even decreases  $\Delta G$ . In addition, there would be inhomogeneous stress distribution in the polymer [27,28], introducing error in the evaluation in  $\Delta G$ . For further quantitative interpretation, detail knowledge of the energy states in both crystal forms and microscopic stress distribution are therefore necessary, and these are deserved for the future projects.

### 3.6. Transition regime

In the transition regime, crystals in the  $\alpha$  form turn into the  $\beta$  form under an approximately constant stress of  $\sigma^*$ . The magnitude of the transition regime,  $\Delta\epsilon = \epsilon_e - \epsilon_i$ , is given by Eq. (3) based on a series model [13].

$$\Delta\epsilon_{\text{calc}} = X \{ [(L_\beta - L_\alpha)/L_\alpha] - (\sigma^*/E_\alpha) \} \times 100(\%) \quad (3)$$

where  $\epsilon_i$  and  $\epsilon_e$  denote the strains at the initial and end of the transition, respectively. The  $\Delta\epsilon_{\text{calc}}$  and  $\Delta\epsilon_{\text{obs}}$  denote the estimated and observed values for  $\Delta\epsilon$ , respectively.  $L_\alpha$  and  $L_\beta$  represent the fiber periods of the  $\alpha$  and  $\beta$  form, respectively.  $X = L_{\text{cr}}/L_0$  where  $L_{\text{cr}}$  and  $L_0$  denote the crystal size and the long period of the  $\alpha$  form along the fiber axis, respectively: the authors obtain  $L_{\text{cr}}$  and  $L_0$  to be 9.5 and 11.9 nm, respectively.  $E_\alpha$  denotes the crystal modulus of the  $\alpha$  form. The first term in the right hand side of Eq. (3) represents the strain arising from the difference in the fiber identity period of each crystal form. The second term represents the strain in crystals ( $\alpha$  form) at the initiation of the transition. It has been reported that the value of  $\Delta\epsilon_{\text{calc}}$  calculated from Eq. (3) account well for the  $\Delta\epsilon_{\text{obs}}$  in PBT ( $\Delta\epsilon_{\text{calc}} = 9\%$  and  $\Delta\epsilon_{\text{obs}} = 10\%$ ) [7] and in PTMS ( $\Delta\epsilon_{\text{calc}} = 6.5\%$  and  $\Delta\epsilon_{\text{obs}} = 8\%$ ) [13] as summarized in Table 2. In the case of PES, the strain is obtained to be  $\Delta\epsilon_{\text{calc}} = 10\%$ , with  $X = 0.8$ ,  $L_\alpha = 0.84$  nm,  $L_\beta = 0.95$  nm (per monomer unit),

Table 2  
Parameters of transition regime for PES, PTMS and PBT

Materials	PES	PTMS	PBT
$\Delta\epsilon_{\text{obs}}$	13	8	10
$\Delta\epsilon_{\text{calc}}$	10	6.5	9
$X$	0.8	0.8	0.8
$\sigma^*$ (MPa)	190	140	75
$E_\alpha$ (GPa)	26.5	13.0	13.5

$\sigma^* = 190$  MPa and  $E_\alpha = 26.5$  GPa, which is close to the observed number of  $\Delta\epsilon_{\text{obs}} = 13\%$  (see Fig. 5a).

The  $\beta$  form contains disorder along the fiber axis, contributing to the strain, resulting in underestimation of  $\Delta\epsilon_{\text{calc}}$ . The contribution by the disorder is given by Eq. (4).

$$\Delta\epsilon_{\text{dis}} = \Delta\epsilon_{\text{obs}} - \Delta\epsilon_{\text{calc}} \quad (4)$$

Inserting  $\Delta\epsilon_{\text{obs}} = 13\%$  and  $\Delta\epsilon_{\text{calc}} = 10\%$ , we obtain  $\Delta\epsilon_{\text{dis}}$  to be 3%, indicating that the contribution of the disorder would be 1/4 of the total strain.

## 4. Conclusions

We have investigated the crystal transition mechanisms between the  $\alpha$  and  $\beta$  form in poly(ethylene succinate) (PES) by using FT-IR and X-ray diffraction. In the FT-IR, the absorbance peaks for the  $\alpha$  form (841 and 873 cm<sup>-1</sup>) started decreasing at strain of  $\epsilon \sim 20\%$ , while the absorbance of the  $\beta$  form (805 cm<sup>-1</sup>), appeared at  $\epsilon \sim 20\%$ , then increased with strain. In addition, the isosbestic point was observed at 820 cm<sup>-1</sup>.

In the X-ray diffraction, two well-defined reflection peaks at  $2\theta = 20.4^\circ$  for  $\alpha$  120 and  $2\theta = 21.9^\circ$  for  $\beta$  form were observed. In addition, streaks in layer lines appeared in the  $\beta$  form, indicating that the  $\beta$  form of PES contains disorder along the chain axis. The intensity of the reflection at  $2\theta = 20.4^\circ$  started decreasing at  $\epsilon \sim 15\%$ , while the reflection at  $2\theta = 21.9^\circ$  appeared at  $\epsilon \sim 15\%$  then increases with  $\epsilon$ : the change was reversible with respect to the repeated application and removal of stain. These observations were thus consistent with the FT-IR results. The molar fraction of the  $\beta$  form,  $\chi_\beta$ , was determined as a function of stress,  $\sigma$ , by X-ray, and the  $\chi_\beta$  showed a drastic increase at around  $\sigma^* \sim 190$  MPa. These observations indicated that the thermodynamic first-order phase transition was the operative mechanism of the transition as similar to those reported in PBT and in PTMS. The free energy difference between the  $\alpha$  and  $\beta$  form,  $\Delta G$ , was estimated to be  $\Delta G \sim 2.3$  (kJ/mol of monomer unit), which is somewhat greater than those observed in PBT ( $\Delta G \sim 1.4$ ) and in PTMS ( $\Delta G \sim 1.6$ ) due to the difference of conformational change during the transition.

## Acknowledgements

This research was partially supported by a Grant-in-aid for Scientific Research (09750984) from the Ministry of Education, Science, Sports and Culture of Japan.

## References

- [1] Boyle CA, Overton JR. Bull Am Phys Soc 1974;19:352.
- [2] Jakeways R, Ward IM, Wilding MA, Hall IH, Desborough IJ, Pass MG. J Polym Sci Polym Phys Ed 1975;13(4):799–813.

- [3] Lu FM, Spruiell JE. *J Appl Polym Sci* 1986;31(6):1595–607.
- [4] Yokouchi M, Sakakibara Y, Chatani Y, Tadokoro H, Tanaka T, Yoda K. *Macromolecules* 1976;9(2):266–73.
- [5] Hall IH, Pass MG. *Polymer* 1976;17(9):807–16.
- [6] Siesler HW. *J Polym Sci, Polym Lett Ed* 1979;17(7):453–8.
- [7] Tashiro K, Nakai Y, Kobayashi M, Tadokoro H. *Macromolecules* 1980;13(1):137–45.
- [8] Roebuck J, Jakeways R, Ward IM. *Polymer* 1992;33(2):227–32.
- [9] Perry BC, Koenig JL, Lando JB. *Macromolecules* 1987;20(2):422–7.
- [10] Brereton MG, Davis GR, Jakeways R, Smith T, Ward IM. *Polymer* 1978;19(1):17–26.
- [11] Davis GR, Smith T, Ward IM. *Polymer* 1980;21(2):221–5.
- [12] Ichikawa Y, Suzuki J, Washiyama J, Moteki Y, Noguchi K, Okuyama K. *Polymer* 1994;35(15):3338–9.
- [13] Ichikawa Y, Washiyama J, Moteki Y, Noguchi K, Okuyama K. *Polym J* 1995;27(12):1230–8.
- [14] Ichikawa Y, Kondo H, Igarshi Y, Noguchi K, Okuyama K, Washiyama J. *Polymer* 2000;41(12):4719–27.
- [15] Chatani Y, Hasegawa R, Tadokoro H. *Polym Prep Jpn* 1971:420.
- [16] Ueda AS, Chatani Y, Tadokoro H. *Polym J* 1971;2(3):387–97.
- [17] Ichikawa Y, Washiyama J, Moteki Y, Noguchi K, Okuyama K. *Polym J* 1995;27(12):1264–6.
- [18] Tashiro K, Tadokoro H. *Rep Prog Polym Phys Jpn* 1978;21:417–20.
- [19] Alexander LE. *X-ray diffraction methods in polymer science*. New York: Wiley, 1969.
- [20] Jakeways R, Smith T, Ward IM, Wilding MA. *J Polym Sci, Polym Phys Ed* 1976;14(1):41–46.
- [21] Yokouchi Y, Chatani Y, Tadokoro H, Teranishi K, Tani H. *Polymer* 1973;39(14):267–72.
- [22] Chatani Y, Okita Y, Tadokoro H, Yamashita Y. *Polym J* 1970;1(5):555–62.
- [23] Tsujimoto J, Murakami S, Tsuji M, Kohjiya S. *Sen'i Gakkaishi* 1999;55(8):361–8.
- [24] Tsuji M, Tsujimoto J, Murakami S, Kohjiya S. *Sen'i Gakkaishi* 1999;55(11):511–21.
- [25] Ciferri A. *Trans Faraday Soc* 1963;59:562–9.
- [26] Feughelman M. *J Appl Polym Sci* 1966;10(12):1937–47.
- [27] Tashiro K, Wu G, Kobayashi M. *Polymer* 1988;29(10):1768–78.
- [28] Takayanagi M, Imada K, Kajiyama T. *J Polym Sci C* 1966;15:263–80.